Influence of SSA and Particle Size Distribution of Iron Oxide on Magnetic Properties of Mn-Zn Ferrite

Y. H. HUNG, P. W. CHEN, C. C. HUANG and M. F. KUO

New Materials Research & Development Department
China Steel Corporation

In this work, Fe_2O_3 powders with different industrial specific surface area (SSA) made by different processes including spray roasting and fluidized-bed process have been prepared. The SSA, particle size distribution, sintering reactivity, solid state reaction as well as magnetic properties of MnZn ferrite for iron oxides are comprehensively investigated.

The results show that the primary particles size distribution of iron oxides made by the fluidized-bed process are sharp and less aggregated than that by the spray roasting process, which results in low temperature formation of $ZnFe_2O_4$. The primary particles of the fluidized-bed Fe_2O_3 is around 0.2~0.3μm, which contributes to the highest green density and the highest sintered density without abnormal grain growth. The sintered parts of iron oxides processed by the spray roasting process trigger the grain growth from 95% theoretical density, as well as wet milled SB-Fe_2O_3 of China Steel Corporation (CSC). However, iron oxides by the fluidized-bed process sustain 98% theoretical density without abnormal grain growth due to the tight particle size distribution with well-controlled particle sizes smaller than 44μm. High SSA of Fe_2O_3 shows high spinel formation with expansion and the lowest peak temperature of expansion. Iron oxides with SSA of 4~4.5m^2/g reveal the lower hysteresis loss (P_h) and the initial permeability enhances with the increase of SSA for low loss MnZn ferrites.

Keyword: Iron oxide, Specific surface area (SSA), Ruthner Spray roasting, Lurgi fluidized-bed

1. INTRODUCTION

The raw material of Fe_2O_3 powder with different chemical and physical properties is undoubtedly important for the MnZn ferrite manufacturing process. In order to obtain either low magnetic power losses or high magnetic permeability of MnZn ferrites for low or high frequency applications, the iron oxide with high chemical purity for the preparation is necessary.[1,2] However, by using a conventional process to manufacture the MnZn Ferrites, the influence of iron oxide supplied by Ruthner spray roasting and Lurgi fluidized-bed process are less studied.

The present study was taken as part of the program to evaluate the iron oxides powders in the fabrication of ferrites as well as the iron oxides supplied by Ruthner spray roasting and Lurgi fluidized-bed process.

2. EXPERIMENT

In this work, different specific surface area (SSA) of industrial Fe_2O_3 powders, including made by Ruthner spray roasting and Lurgi fluidized-bed process, were studied. Ferrites prepared by different Fe_2O_3 powders were investigated based on the SSA, particle size distribution, sintering activity, and solid state reaction. The different SSA iron oxides from a different supplier designated as SB-Fe_2O_3 (SSA=3.4 m^2/g) and SA-Fe_2O_3 (SSA=4.19 m^2/g) from China Steel Corp. (CSC), C9-Fe_2O_3 (SSA=4.78 m^2/g), C6-Fe_2O_3 (SSA=5.52 m^2/g) from C supplier, and NM-Fe_2O_3 (SSA=5.18 m^2/g) and NH-Fe_2O_3 （SSA=5.94 m^2/g） from N supplier. Part of SB-Fe_2O_3 was wet milled by attritor. Iron oxides of SA, SB, NH and NM were manufactured by Ruthner spray-roasting process, and the C6 and C9 iron oxides were made by Lurgi fluidized-bed process. Chemical analysis of iron oxides was performed with an Agilent Axial 720 ICP-emission spectroscopy. The BET was determined by nitrogen absorption using Micrometrics. Particle size analysis was performed on ultrasonically treated aqueous dispersions of the oxides by laser scattering, using COULTER LS.

All iron oxides were uniaxial pressed in to a die of 2 mm height and 15 mm diameter at a pressure of 100 MPa. Sintered samples were quenched in water after being fired at the rate of 5°C/min. from 700°C to 1300°C for a duration of 5 minutes. Microstructures were observed by optical microscopy and SEM. Grain size was measured by an intercept method.

Zinc ferrite was chosen as a typical ferrite to evaluate the Fe_2O_3 raw material powders in the fabrication

process of ferrite cores. The iron oxides with different SSA and zinc oxides were dry mixed in an agitator at 3000 rpm for 30 seconds. All mixtures were uniaxial pressed in to a die of 2 mm height and 15 mm diameter at a pressure of 100 MPa. Sintered samples were quenched in water after firing at 5°C/min. from 600°C to 1000°C for 5 minutes duration time. Microstructures were observed by optical microscopy and SEM. The spinel to hematite ratio after firing was estimated with X-ray diffraction (XRD, Cu-Kα radiation) for phase identification of the calcined samples. Grain size was measured by intercept method.

The formula of MnZn ferrite of high permeability M10 (10000μi) and power ferrite (MZ4) powder were prepared by mixture of weighted proportions of Fe_2O_3, Mn_3O_4 and ZnO. The milled powders were subsequently granulated with PVA and compacted towards toroidally shaped specimens at a pressure of 100 MPa. The magnetic properties of controlled atmosphere sintered MnZn ferrite cores were measured by Iwatsu 8232 BH analyzer. The initial permeability (μi) and loss factor were performed at a frequency of 100 KHz, a magnetic induction level of 0.5 A/m, and the power loss (PL) done at a frequency of 100 KHz, a magnetic induction level of 200mT. μi, LF and PL of all ferrite cores were measured between 25~120°C with intervals of 20°C. The geometric mean of μi, LF and PL of measured temperature were sometimes represented as the magnetic properties.

3. RESULTS AND DISCUSSION

3.1. Evaluation of iron oxides

The chemical and physical properties of iron oxides in this study are shown in Table 1. The impurity of phosphor (P) in iron oxides shows nearly the same quantity. The concentrations of Cr and Al of iron oxide powder from CSC are lower than that of N supplier, but are nearly equal to C supplier. The impurities of Ni and Cl in SA and SB Fe_2O_3 are higher than those of N supplier and are nearly equal to those of C supplier, but the content of Cl is lower than C supplier[3].

The particle size and D50 of Fe_2O_3 powder from CSC is larger than that of both C and N suppliers. The SSA of Fe_2O_3 powder is the lowest from CSC. The BD is also lower but the CD is higher than that of N supplier.

From the above experimental results, it is believed that the chemical purity of Fe_2O_3 powder from CSC is better than that of N supplier and nearly equal to that of C supplier. However, the lower SSA and larger particles were also observed in SA and SB Fe_2O_3 powder.

The particle size distribution of different iron oxides is shown In Fig.1 (a). Fe_2O_3 powder from CSC has a wider distribution compared to the others. Iron oxides from C supplier shows a narrow particle size distribution

Table 1 The chemical and physical properties of iron oxides in this study

	CSC		C 公司		N 公司	
	SB	SA	C9	C6	NH	NM
SO_2 (ppm)	75	79	85	118	41	72
Ca (ppm)	60	60	74	74	32	40
Mn (ppm)	2200	2300	2308	2569	2478	2335
Al (ppm)	12	22	15	17	101	37
P (ppm)	15	15	15	14	15	16
Cu (ppm)	10	10	7	6	3	13
Ni (ppm)	90	106	94	112	58	76
Cr (ppm)	8	4	6	6	22	17
Cl (%)	0.07	0.09	0.11	0.13	0.04	0.04
Na (ppm)		--	25	21		
Aps (μm)	0.85	0.75	0.65	0.60	0.70	0.72
BD (g/cm^3)	0.52	0.50	0.50	0.50	0.79	0.78
CD (g/cm^3)	2.75	2.72	2.85	2.85	2.71	2.67
D_{50} (μm)	7.5	---	2.286	2.286	2.452	2.178
SSA (m^2/g)	3.4	4.19	5.52	5.52	5.94	5.18
篩殘率 (%)	1.782	0.763	0	0	8	---

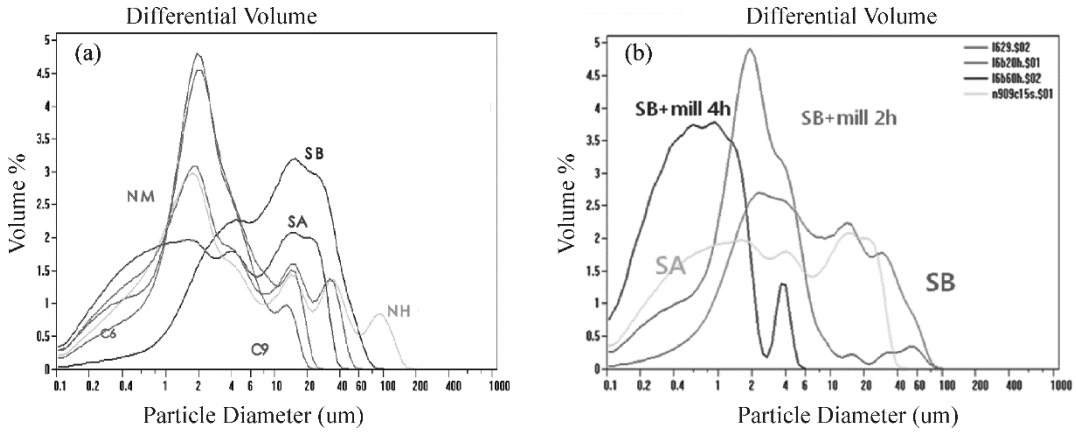

Fig.1. (a) The comparison of particle size distribution for iron oxides and (b) milled and non-milled of SB-Fe_2O_3

with a particle size of below 40μm and without aggregation. However, iron oxides from C and N supplier contain more ≦1μm particles, but NH iron oxide also shows more ≧100μm particles accompanied with agglomerates or aggregates.[4]

SB-Fe_2O_3 powder was intensively wet milled by attritor for 2 and 4 hours to verify the influence on sintering reactivity. Figure 1(b) and table 2 illustrates that the high SSA associated with finer particle size and sharper particle size distribution was obtained by increasing the milling time. Although coarse particle size reduces after 2 hours wet milling, it still exhibits nearly the same particle size distribution band-width. This infers that SB-Fe_2O_3 powder might have some sinter reaction during the spray roasting process.

3.2. Sintering activity of iron oxides

Figure 2 is the green density of different SSA of iron oxides. The result exhibits lower green density of compacted iron oxide for higher SSA of iron oxide powder. Lower green density of finer particle (higher SSA) of iron oxide results from the finer pore in the green body and more friction during compaction. Iron oxides with narrower size distribution (C6&C9) that were manufactured by Lurgi fluidized-bed process show higher green density. The Green body of milled SB iron oxides also show higher green density.

Figure 3. is the shrinkage behavior of different iron oxides as well as those with milling. Iron oxides from N supplier begin shrinkage behavior at a lower temperature and show the highest shrinkage ratio. Iron oxides from CSC with larger particle size (SA&SB) have sluggish shrinkage behavior and with lowest overall shrinkage. The early stage shrinkage of sintering is explained by rapid sintering of < 1μm particles followed with the disappearance of the small pore. Therefore, NM, NH, C6 with a large green body and small pore have a high shrinkage rate at the early stage. The temperature at the beginning of the shrinkage trend is NM≒NH≒C6≒C9 ＜SA＜SB. The shrinkage rate at 1300℃ is C9＞NH＞C6＞NM＞SA＞SB. The milled SB iron oxides exhibit a large shrinkage rate below 1000℃ during sinter but have the lowest shrinkage rate at a the higher temperature because of the duplex structure of the sintered body.

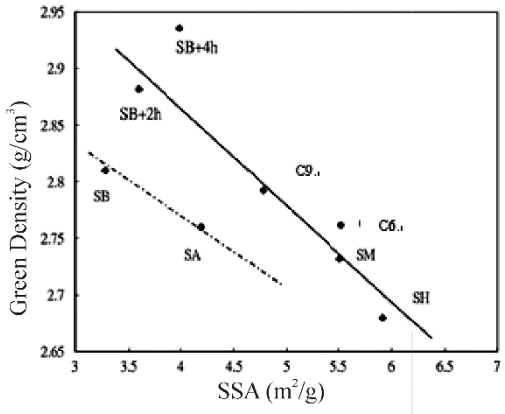

Fig.2. The green density of different SSA of iron oxides

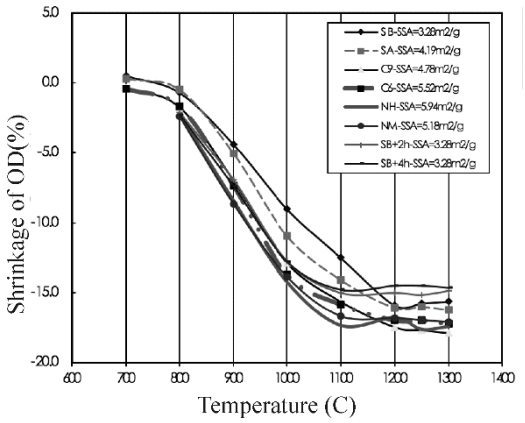

Fig.3. The shrinkage behavior of different SSA of iron oxides

The grain size and sintered density for different SSA of iron oxides at different sintering temperatures are shown in Fig.4. C6 and C9 iron oxides made by Lurgi fluidized-bed process show a significant grain growth from 98% of theoretical density. The narrow particle size distribution is better than those of by the Ruthner spray-roasting process from 95% theoretical density. A higher densification rate in the beginning, but a wide particle size distribution hinder subsequent densification that belong to NH and NM iron oxide which are characterized by higher SSA and more <1μm particles. These results infer that the densification mechanism in iron oxides from the Ruthner spray- roasting process is not the same as that for Lurgi fluidized-bed process.

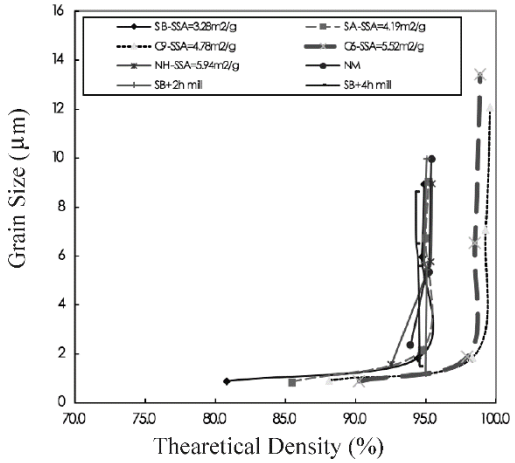

Fig.4. The grain size and sintered density for different SSA of iron oxides at different sintering temperature

In Fig.4, SB iron oxide with a wide particle size distribution shows the grain growth at 95% theoretical density. Even premilled SB iron oxide exhibits finer particle size, higher SSA and sharper size distribution with increased milling time. It implied that SB-Fe_2O_3 powder suffers sintering during the spray roasting process. Even 2 hours of intensive wet milling brings nearly the same particle size distribution band-width that retards the densification.

Nomura etc. suggests that densification behavior does not show any clear dependence on primary particle size but is affected by the aggregation state. Extensive pore growth and broad distribution of open-pore size was observed in aggregated powder.[5~8] The retardation of densification of iron oxide made from Ruthner spray-roasting process has a broad size distribution together with broad pore size. Premilled SB iron oxide does not change the particle size distribution band-width and also retards the densification. The wide particle size (Fig.1) distribution shows lower green density (Fig.2) due to increased pore and poor pore size distribution, which plays an important role on grain growth only at 95% theoretical density.

Zheng concludes that fine pores (pore size <1/2 particle size) are first eliminate and only fine micro pores can be totally eliminated. The porosity of coarse micropore (1/2 particle size <pore size < 10 times of particle) may increase due to pore coalescence, and macroporosity is unchanged because their shrinkage is that of the whole compact.[9] C supplier manufactured iron oxides with narrow particle size distribution by Lurgi fluidized-bed process which implies narrow pore size distribution which sintered body grain grows until 98% theoretical density.

3.3. Magnetic properties of the high permeability M10 (10000μi) and power ferrite (MZ4) of Mn-Zn ferrites from different SSA of iron oxides

The initial permeability (μi) of power ferrite (MZ4) with the lowest power loss ($PL_{100KHz,0.2T}$) at 4~4.5m^2/g (Fig.5(a)) increases with the increase of the SSA of iron oxide. Permeability increases with grain size without trapping pores for high purity and sintering activity of iron oxide. Since PL depends on eddy current loss, hysteresis loss and a ferrite core of appropriate grain size are

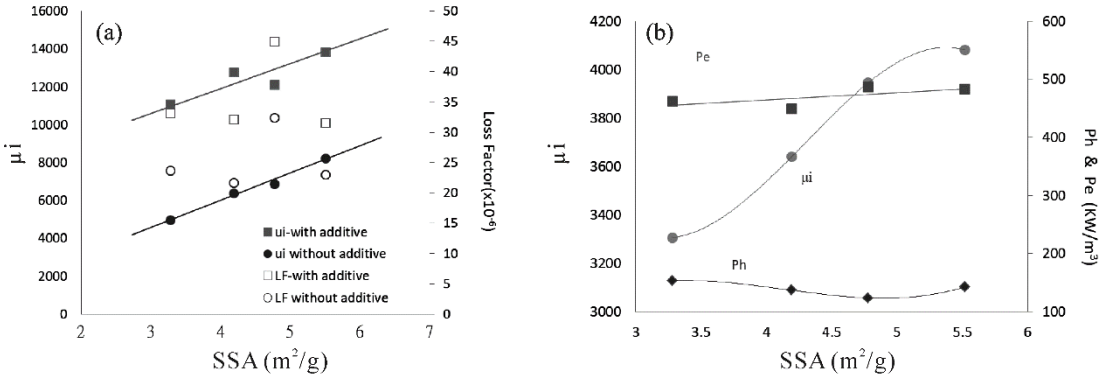

Fig.5. (a) The magnetic properties of MZ4 power ferrite and (b) high permeability M10 ferrite for various iron oxides

required. Moreover, the 4.5~5.0m^2/g of Fe_2O_3 is well packed with other raw materials. Consequently, lower hysteresis loss (Ph) is achieved. However, the eddy current loss (Pe) is independent of the SSA of Fe_2O_3.

Figure 5(b) shows the variation of μi and the loss factor (LF) with SSA of iron oxides for a high permeability (M10) ferrite core. The μi of M10 ferrite increases with the increase of SSA of iron oxide, and μi of M10 ferrite increases with flux additive compared to cores without additive. However, no relationship was observed between the loss factor (LF) and SSA. The μi increases with grain size without trapping pores for high purity, homogenous mixing and sintering activity of iron oxide without > 40μm particle size.

The magnetic properties of MZ4 power ferrite for milled and non-milled SB-Fe_2O_3 oxides are shown in Fig.6. The MZ4 powder ferrite used was pre-milled for 4h, the SB-Fe_2O_3 powder has the highest μi and lowest PL. It is believed that SB-Fe_2O_3 powder suffers sintering during the spray roasting process. Even under 2 hours intensive wet milling brings nearly the same band-width of particle size distribution that hinders the densification. However, pre-milled 4h SB-Fe_2O_3 powder with higher SSA and narrow particle size distribution bring higher sintering activity for ferrite.

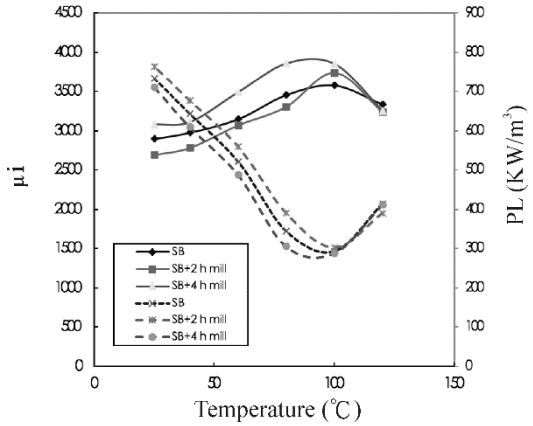

Fig.6. The magnetic properties of MZ4 power ferrite for milled and non-milled SB-Fe_2O_3 oxides

The μi of M10 ferrite core decreases with increasing SSA of SB iron oxide for longer pre-milling times (shown in Table 2 and 3). However, loss factor (LF) shows the opposite tendency. M10 ferrite core sintered at 1360°C for 4h is a crucial process sequence for 95% theoretical density to initiate abnormal grain growth, which is different to MZ4 only with a lower sintering temperature of 1320°C for 2 h[10]. A longer pre-milling time favours an increase in <1μm particles, which will lead to the occurrence of easily abnormal grain growth under a higher sintering temperature of 1360°C for 4 h.

4. CONCLUSIONS

1. Iron oxides from C supplier by Lurgi fluidized-bed process possess well-controlled <40μm particles and tight particle size distribution. The tendency of particles are towards C6 < C9 < NH < NM < SA < SB.
2. Although coarse particle size decreases after 2 hours wet milling, the particle size distribution band-width is nearly the same. This implies SB-Fe_2O_3 powder has some sinter reaction during the Ruthner spray roasting process.
3. Iron oxides with narrow size distribution manufactured by Lurgi fluidized-bed process show signficant grain growth from 98% theoretical density. However, other conditions processed by Ruthner spray- roasting process show the beginning point of grain growth at 95% theoretical density. The compact body of pre-milled SB iron oxide also begin grain growth at 95% theoretical density, even exhibiting finer particle size, higher SSA and sharper size distribution as milling time increases.
4. The μi of power ferrite increases as SSA of iron oxide increasing, but 4.5~5m^2/g of Fe_2O_3 is well packed with other raw materials; consequently, lower hysteresis loss (Ph) is achieved. However, the eddy current loss (Pe) is independent to the SSA of Fe_2O_3.
5. The μi of M10 ferrite decreases and loss factor increases as pre-milling time increases.

Table 2 The comparison of SSA of milled and non-milled SB-Fe_2O_3 and SA-Fe_2O_3

	SB Non milled	SB milled 2 hr	SB milled 4 hr	SA
SSAm2/g	3.09	3.60	3.99	4.19

Table 3 The magnetic properties of M10 ferrites core for milled and non-milled SB-Fe_2O_3

	SB	SB milled 2hr	SB milled 4hr
i	12380	10333	10239
LF	12.57	14.67	15.24

REFERENCES

1. A. Goldman, Handbook of modern ferromagnetic materials, Ferrite Processing, Kluwer Academic publishers, USA, (1999) 305-308.
2. M. F. Yan, D. W. Johnson Jr., Impurity induced exaggerated grain growth in MnZn ferrites, J. Am. Ceram. Soc. 61 (1978) No. 7-8, 42-349.
3. Y. H. Hung and C. L. Huang, Bulletin of Powder Metallurgy Association, Taiwan, Vol. 36, No. 3, p. 1, 2011.
4. W. F. M. Groot Zevert, A. J. A. Winnubst, A. J. Burggraaf, J. Mater. Sci. 25 (1990), 3449-3455.
5. T. Yamaguchi and T. Nomura, J. Jpn. Soc. Powder powder Metall., 26 (1979), No. 7, 12.
6. T. Yamaguchi and T. Nomura, J. Jpn. Soc.Powder powder Metall., 26 (1979) , No.7, 18.
7. T. Yamaguchi and T. Nomura, J. Jpn. Soc.Powder powder Metall., 29 (1982), No. 1, 13.
8. T. Yamaguchi and T. Nomura, J. Jpn. Soc. Powder powder Metall., 29 (1982), No. 1, 8.
9. J. G. Zheng and J Reed, Am. Ceram. Bull., 71 (1992) No. 9, 1410.
10. Y.H. Hung, P.W. Chen, S. W. Yeh and Y.R. Tseng,WORLDPM2018, Sept. 16-20, Beijing China. □